

THE COLOR-ABSOLUTE MAGNITUDE RELATION FOR E AND S0 GALAXIES. II. NEW COLORS, MAGNITUDES, AND TYPES FOR 405 GALAXIES

ALLAN SANDAGE

Hale Observatories, Carnegie Institution of Washington, California Institute of Technology

AND

NATARAJAN VISVANATHAN

Hale Observatories, Carnegie Institution of Washington, California Institute of Technology; and Mount Stromlo and Siding Spring Observatories, Research School of Physical Sciences, Australian National University

Received 1977 November 4; accepted 1978 February 10

ABSTRACT

Multicolor and multiaperture photometry in a new u, b, V, r system, standard V_{26} magnitudes, new types, and velocities are listed for 405 E, S0, SB0, S0/a (and a few Sa) galaxies. Corrections for the effects of color and magnitude variations with aperture are derived. Average colors reduced to $\theta/D(0) = 0.5$, and standard V_{26} magnitudes reduced to $\theta/D(0) = 2.5$, are also given for each galaxy.

The existence of a color gradient across the face of many galaxies is seen in our data. Colors are generally redder toward the nucleus. The gradients show a strong wavelength dependence, similar to the C-M effect itself. The mean gradients are the same for E and S0 galaxies separately and show no dependence on absolute magnitude in the range $-20 < M_V < -24$.

Differentiation of the color-aperture effect gives an average variation of $\Delta(u - V) = 0.15$ mag in the surface color over the interval $0.1 < \theta/D(0) < 1.0$. This variation can be explained by an outward decrease in mean metal abundance in the disks and halos by a factor of ~ 2 over the stated diameter interval.

The mean Galactic reddening obtained from the data is smaller by a factor of 2 in $b - V$, $V - r$, and $u - V$ than values based on galaxy counts, but is consistent with other recent determinations from colors of high-latitude stars and globular clusters.

The C-M effect is shown to be the same for field E and S0 galaxies as for cluster and group members. Hence the effect may be universal and, further, the present data provide no evidence for differences in the stellar content of early-type galaxies that depend on their environment.

Subject headings: galaxies: photometry — galaxies: structure

I. INTRODUCTION

We began a photometric program in 1973 to observe most of the E and S0 galaxies in the Shapley-Ames catalog (1932). The observations of 405 galaxies were made in the u, b, V, r system described in Paper I (Visvanathan and Sandage 1977). The aim is to obtain independent distances to a large homogeneous sample of group and field galaxies in the local region. This sample, combined with data for nearby early- and late-type spirals (Sandage and Tammann 1975; Visvanathan and Griensmith 1977) may eventually permit a measurement of the velocity perturbations of field galaxies caused by density contrasts of nearby clumps (Sandage, Tammann, and Hardy 1972; Silk 1974; Peebles 1976), from which the local value of the deceleration parameter q_0 would follow. It is important to note that this and other local tests of the cosmological model entirely avoid the problems of evolutionary effects because of the short look-back time, and are therefore very powerful.

The colors and magnitudes of the galaxies were measured in the manner described in Paper I, using

the telescopes at Palomar and at Las Campanas. Radial velocities for galaxies with unknown redshifts were measured at Mount Stromlo between 1969 and 1972, and at Palomar since 1970. New galaxy types were also obtained from large-scale reflector plates from Mount Wilson, Palomar, and Las Campanas, and from Uppsala Schmidt plates taken at Mount Stromlo.

In this paper, we present these data for the program galaxies. This is followed by a discussion of the color-aperture effect for E and S0 galaxies, the K -reddening due to redshift, and the aperture correction to V magnitudes. An average standard corrected color, reduced to $\theta/D(0) = 0.5$, and a standard V magnitude reduced to $\theta/D(0) = 2.5$ are given for each galaxy. Galactic reddening as a function of b is derived from the corrected color data.

Finally, a demonstration is given that the C-M relation, established in Paper I for the Virgo cluster and nine other nearby groups and clusters, applies equally to the present sample of E and S0 field galaxies. Hence, whatever the cause of the C-M effect, it appears to be universal, and may be useful for the

determination of relative distances to galaxies in clusters, groups, and in the general field.

II. DATA

a) The Sample

Of the 394 galaxies of types E, S0, SB0, or SB0/a in the Shapley-Ames catalog of 1246 bright galaxies, we have obtained photoelectric data for 323, which is 83% of the total. An additional 82 galaxies have been observed, some of which are in the Shapley-Ames catalog but are of later type, and some are fainter than the catalog limit. A total of 405 galaxies are in the final sample.

The projected distribution of these galaxies in galactic coordinates is shown in Figure 1. Hubble's (1934) zone of avoidance is sketched, and the number of low-latitude galaxies makes it again possible to study the galactic reddening (§ VI).

b) Instrumentation and Observational Procedure

The automatic scanner with a digital recording system (Visvanathan 1972; Paper I; Visvanathan and Griensmith 1977) was used in a single-channel mode for all the observations. An ITT FW130, S20 photomultiplier was used with an SSR 50 MHz preamplifier.

The filter wheel containing the u_1 , u_2 , b , V , and r filters described in Paper I was rotated by a stepping motor that was programmed to dwell for predetermined times at each filter position. The exposures through the filters were 128, 128, 12, 12, and 24 units of 15.5 ms, respectively. The total time for a single scan was kept at 6 seconds. To maintain control of the sky variations, the number of the scans for any one observation was kept to 16 or 32, and the galaxy observation was always preceded and succeeded by the sky.

The net galaxy count was converted into magnitude and reduced to outside the atmosphere using average extinction coefficients for each color. A description of the instrument, recording system, and the observing and reduction procedures is given in Paper I.

The scanner was used at the Cassegrain foci of the 1.5 m and 5 m reflectors at Palomar, and the 1 m Swope reflector at Las Campanas. The diameters of the focal plane apertures were 14"9, 30"1, 60"1, and 84"6 at the Palomar 1.5 m, and 1% smaller for the Las Campanas telescope.

c) The Color System

The data were obtained through the medium-band interference filters u_1 , u_2 , b , and r and a conventional broad-band V filter. The transmission curves of the interference filters were folded with a typical S20 photomultiplier response, a giant E galaxy continuum, and one Earth's atmosphere to derive the effective wavelengths of $\lambda\lambda 3466$, 3625, 4522, and 6738 Å for the u_1 , u_2 , b , and r filters, respectively. The effective wavelength for the V filter (GG14 + BG18) is 5400 Å.

In the reduction, intensities through the two ultraviolet filters u_1 , u_2 were added to form a single u point

TABLE 1

ADOPTED VALUES FOR THE 13 STANDARD STARS

Name	V	$b - V$	$V - r$	$u - V$
HD 19445...	8.00	+0.21	0.22	1.04
HD 84937...	8.29	+0.15	0.16	1.05
HD 140283...	7.22	+0.22	0.30	1.10
HD 183143...	6.87	+0.80	0.87	2.18
M67-81.....	10.03	-0.24	0.02	0.49
M67-105.....	10.30	+0.81	0.80	3.34
M3-1402.....	12.66	+0.33	0.31	1.57
M92-114.....	13.83	+0.56	0.46	2.07
HD 225233...	7.30	+0.19	0.22	1.34
HD 213785...	7.77	+0.10	0.16	1.17
HD 24249...	7.35	-0.05	0.00	1.29
HD 106456...	7.57	+0.64	0.61	2.82
HD 151415...	7.10	+1.16	1.15	4.57

at $\langle \lambda \rangle \approx 3550$ Å with $\Delta \lambda \approx 250$ Å. The resulting $ubVr$ system gives colors $u - V$, $b - V$, and $V - r$ and a visual magnitude V which we reduced to the standard Johnson and Morgan (1953) scale and zero point. The zero points in color are defined by 13 standard stars whose adopted values are given in Table 1. These standard stars were observed many times during the three observing seasons.

d) Observed $ubVr$ Data for Program Galaxies

The adopted photometric data for the 405 galaxies are listed in Table 2. They have been reduced to a final homogeneous photometric system by night corrections determined from the complete material at the end of the program.

The NGC galaxies are listed first in column (1). Twenty-two IC galaxies, two anonymous systems, and two faint galaxies in the Coma cluster (listed by their Rood-Baum [1967] numbers) are given at the end of the table. Column (2) gives the new galaxy types, on the system of the Hubble Atlas (Sandage 1961). The notation is standard, except that the ellipticity $10(a - b)/a$ is listed in parentheses for S0 galaxies. The types are new and are internally homogeneous. They were determined over a short time from the available large reflector plates at the Mount Wilson and Palomar Observatories, and supersede those listed in Humason, Mayall, and Sandage (1956, hereafter HMS).

Column (3) lists the telescopes used in the photometry. P60 is the Palomar 1.5 m telescope, P200 is the 5 m Hale reflector, and C40 the Swope 1 m reflector at Las Campanas, Chile. Column (4) is the diameter of the measuring aperture in arcsec.

Column (5) gives the aperture ratio $\theta/D(0)$, using the reduced $D(0)$ diameters from the *Reference Catalogue of Bright Galaxies* (de Vaucouleurs and de Vaucouleurs 1964; hereafter RCBG). Columns (6)–(9) give the V magnitude and the colors $u - V$, $b - V$, and $V - r$, respectively. Colons mark the data with larger errors due to insufficient statistics. Parentheses mark values that are suspect, due either to poor skies for the particular observation, or to an occasional malfunction of the rotating filter wheel in the scanner

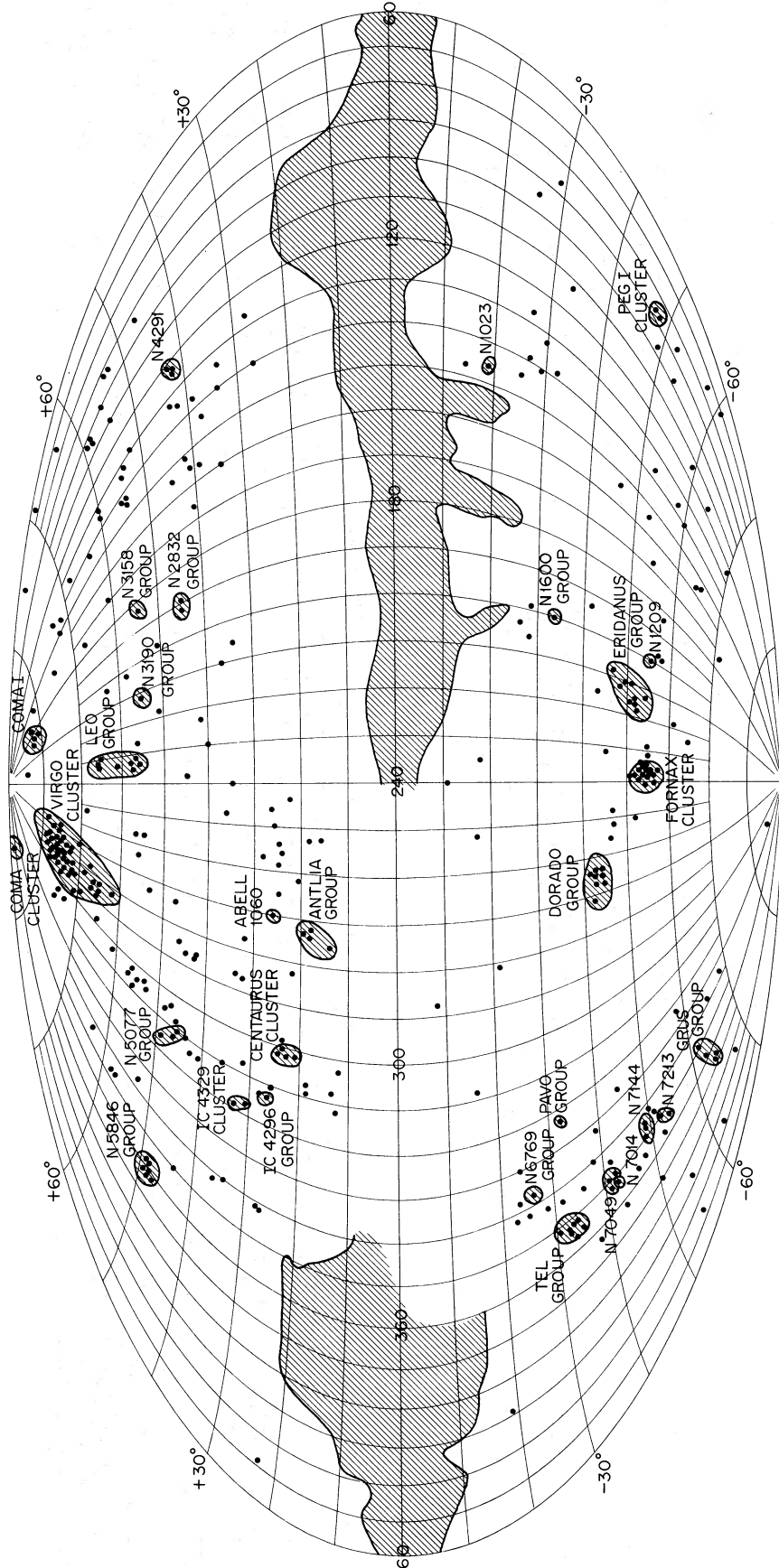


FIG. 1.—Distribution of the present sample of 405 galaxies in galactic coordinates. Groups, as indicated in Table 3, are enclosed in boundaries. The zone of avoidance from Hubble (1934) is outlined approximately.

TABLE 2—Continued

Name (1)	Type (2)	Tel (3)	θ'' (4)	$\theta/D(0)$ (5)	V (6)	$u - V$ (7)	$b - V$ (8)	$V - r$ (9)	Name (1)	Type (2)	Tel (3)	θ'' (4)	$\theta/D(0)$ (5)	V (6)	$u - V$ (7)	$b - V$ (8)	$V - r$ (9)
N7507	EO	C40	7'.6	0.11	13.81	2.50:	IC 1459	E4	C40	59'.5	0.62	10.84	2.47	0.60	0.54
		C40	29.8	0.44	11.59	2.44	0.61	0.60			C40	83.7	0.87	10.64	2.42	0.60	0.52
		C40	59.5	0.88	11.17	2.43	0.64	0.62	IC 2006	E1	C40	29.8	0.40	12.46
		C40	83.7	1.24	10.98	2.45	0.62	0.56	IC 2035	E4:	C40	59.5	0.40	11.85	1.90	0.42	0.38
N7562	E2	P60	14.9	0.27	12.92	2.44	0.65	0.61			C40	59.5	0.40	11.82	1.90	0.37	0.37
N7576	Sa or SO ₃ :	P60	30.1	0.63	13.26	2.20:	0.57:	0.56:	IC 2056	Giant H II?	C40	29.8	0.44	12.55	1.24	0.28	0.57
N7585	SO ₁ (3)/Sa	C40	29.8	0.34	12.56	2.29:	0.55:	0.54:	IC 3370	E2	C40	29.8	0.34	12.40	2.56	0.66	0.61
		P60	30.1	0.35	12.53	2.40	0.64	0.46			C40	59.5	0.67	11.85	2.50	0.64	0.58
		P60	30.1	0.35	12.54	2.33	0.59	0.47	IC 3896	E1	C40	29.8	0.42	12.58	2.60	0.71	0.69
		P60	60.1	0.69	12.04	2.34	0.58	0.50	IC 3998	SB(0)	P200	14.4	0.61	15.16	2.37	0.75	0.57
		P60	60.1	0.69	12.00	2.32	0.57	0.47	IC 4011	EO	P200	10.2	0.84	15.42	2.08	0.59	0.50
N7600	SO ₁ (5)	C40	29.8	0.47	12.91	2.22	0.52	0.48	IC 4012	E3	P200	14.4	1.21	15.51	2.14	0.62	0.50
		C40	59.5	0.95	12.44	2.26	0.55	0.52	IC 4026	SBO	P200	10.2	0.53	15.50	2.25	0.66	0.53
N7617	E6	P60	14.9	0.33	14.70	2.15	0.64	0.72	IC 4042	SBO	P200	14.4	0.38	14.75	2.28	0.66	0.51
N7619	E3	P60	30.1	0.44	12.33	2.58	0.68	0.57	IC 4296	EO	C40	59.5	0.40	11.63	2.48	0.65	0.58
N7626	E1	P60	14.9	0.24	12.98	2.51	0.62	0.61			C40	83.7	0.56	11.39	2.45:	0.64:	0.61:
		P60	14.9	0.24	13.24	2.59:	0.65:	0.60	IC 4327	SO ₁ (5)/E5	C40	29.8	0.34	13.02
		P60	30.1	0.48	12.52:	2.49	0.65:	0.58:	IC 4797	E6/SO ₁ (6)	C40	14.8	0.21	12.84	2.63	0.66	0.63
N7671	SO ₁ (5)	P60	14.9	0.31	13.11	2.53	0.72	0.62			C40	29.8	0.43	12.09	2.51	0.60	0.54
N7679	GH II or SO _p	P60	14.9	0.25	13.33	1.21:	0.24:	0.71:	IC 4889	E5	C40	29.8	0.43	12.08	2.33	0.59	0.60
N7702	Sa:	C40	29.8	0.34	13.07	2.33:	0.58:	0.57:	IC 5063	E4	C40	14.8	0.24	13.65	2.39	0.86	0.87
		C40	29.8	0.34	13.05	2.32:	0.67:	0.55:	IC 5105	E5	C40	29.8	0.44	12.74	2.41	0.66	0.64
N7743	SBa	P60	30.1	0.22	12.74	2.26	0.58	0.49	IC 5181	SO ₁ (8)	C40	29.8	0.41	12.10	2.30	0.57	0.53
		P60	30.1	0.22	12.69	2.26	0.58	0.46	IC 5267	SO ₁ (4)/Sa	C40	29.8	0.17	12.09
		P60	60.1	0.44	12.19	2.25	0.58	0.44	IC 5269	SO ₁ (7)	C40	59.5	0.84	12.78	2.03	0.57	0.50
		P60	60.1	0.44	12.17	2.14:	0.58:	0.45:	IC 5328	E3	C40	29.8	0.43	12.41	2.36	0.57	0.53
N7744	SO ₁ (3)	C40	29.8	0.39	12.39	2.41:	0.60:	0.51	A 1853	E3	C40	14.8	0.26	13.01
N7785	E5	P60	30.1	0.45	12.40:	2.55:	0.61:	0.59:			C40	14.8	0.26	13.01	2.44	0.61	0.55
N7796	E1	C40	29.8	0.40	12.46	2.44	0.60	0.55	A 2021	SO ₁ (6)/E6	C40	29.8	0.36	12.80	2.17	0.58	0.57
		C40	29.8	0.40	12.43	2.49	0.62	0.57	RB 37	SBO	P200	10.2	1.03	17.22:	1.95	0.59	0.49
IC 1459	E4	C40	29.8	0.31	11.27	2.47	0.61	0.55:	RB 42	SO	P200	14.4	1.06	16.12:	2.21	0.66	0.56

that mixed the timing intervals into the channel analyzer. There are 63 galaxies in the list with colons or parentheses. Further, there are 13 galaxies for which only V observations are given.

e) Mean Error from Multiple Observations

To find the accuracy of the colors, the data have been analyzed for galaxies observed more than once with the same aperture but in different seeing and extinction conditions on different nights. All multiple observations in Table 2 are used to derive the mean error of the various colors. It was found that the variance of a single observation is ± 0.03 mag, ± 0.02 mag, and ± 0.02 mag in $u - V$, $b - V$, and $V - r$, respectively. It is to be noted that these values are comparable with the error from photon statistics which generally are $\sim 2\%$; the agreement indicates the absence of systematic external errors from night to night.

f) Comparison with UBV Colors

Transformations of the $ubVr$ colors to the UBV system, derived from data for the standard stars in Table 1, are

$$U - V = 1.05(u - V) - 0.94, \quad (1)$$

$$B - V = 1.25(b - V) + 0.22. \quad (2)$$

We have neglected HD 24249 in this comparison because its $u - V$ color was unstable with time.

Comparison of our colors with the published literature $U - V$, $B - V$, and $V - R$ values for galaxies in common with the present sample (nearly the same aperture size), gives relations in approximate agreement with those derived from stars (the galaxy comparison gives $U - V = 1.15[u - V] - 1.19$, $B - V = 1.31[b - V] + 0.21$, and $V - R = 1.11[V - r] + 0.29$). The dispersions of the comparisons between our colors and the literature values are $\sigma(U - V) = \pm 0.07$, $\sigma(B - V) = \pm 0.04$, and $\sigma(V - R) = \pm 0.03$.

III. CORRECTIONS FOR THE SYSTEMATIC EFFECTS IN COLORS

Before we can analyze the data in Table 2, the systematic effects caused by the color gradient across the face of the galaxy, K -dimming, and Galactic reddening must be removed. The first two effects are discussed in this section. The Galactic reddening as a function of b is derived in § VI.

a) Color-Aperture Relation

Color gradients across the face of the galaxy have been previously studied most extensively by de Vaucouleurs (1961*b*), Tifft (1963, 1969), and de Vaucouleurs and de Vaucouleurs (1972). The colors are generally redder near the nucleus than in the outlying envelope or disk. De Vaucouleurs and de Vaucouleurs (1972) found that the $U - V$ color variation in the interval $0.2 < \theta/D(0) < 2.0$ could be represented by linear logarithmic gradients with slopes varying from -0.05 to -0.25 for early E to late SO

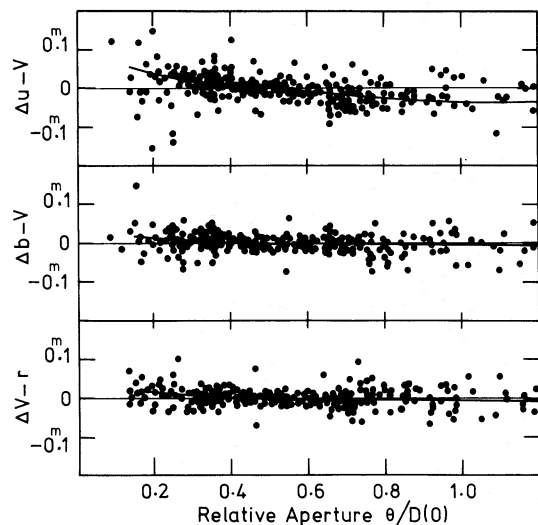


FIG. 2.—Color-aperture gradients in $u - V$, $b - V$, and $V - r$ from data in Table 2, normalized to $\theta/D(0) = 0.5$.

galaxies. The slope in $B - V$ is only one third of that in $U - V$. A similar effect is seen in our data.

Corrections for the observed colors to reduce them to a constant $\theta/D(0) = 0.5$ were derived from the plots of the color differences $\Delta(u - V)$, $\Delta(b - V)$, and $\Delta(V - r)$ versus $\theta/D(0)$ shown in Figure 2. Those galaxies in Table 2 for which multiaperture measurements exist that bracket $\theta/D(0) = 0.5$ were used to compute the color differences relative to the interpolated color at $\theta/D(0) = 0.5$. The mean color variation with $\theta/D(0)$ is indicated by thick lines in the diagram.

Although many galaxies in our sample show neutral or positive color gradients, the individual color differences in Figure 2 are generally within the errors of observations. However, an average negative color gradient in our sample is definite, as given by the mean curve in the range $0.2 < \theta/D(0) < 1.0$. The curves in Figure 2 are closely represented by

$$\Delta(u - V) = -0.10 \log \theta/D(0) - 0.03, \quad (3)$$

$$\Delta(b - V) = -0.03 \log \theta/D(0) - 0.01, \quad (4)$$

$$\Delta(V - r) = -0.03 \log \theta/D(0) - 0.01. \quad (5)$$

The average slopes from equations (3)–(5) in $u - V$ and $b - V$ are less than those in UBV colors (-0.15 in $U - V$, and -0.05 in $B - V$) for E and S0 types (de Vaucouleurs and de Vaucouleurs 1972; Frogel and Persson 1977), due perhaps to a different percentage of galaxies with positive color gradients in the various samples. This fact may be a result of bluer colors than the average near the nucleus for our sample compared with the literature values.¹

¹ The authors note that they have not been able to agree in detail on the proper color-aperture correction to apply. The final corrections to Table 3 follow Visvanathan's precepts of equations (3)–(5). Sandage's conclusions using the same data give closely the same gradient as UBV literature gradients at

It is now of interest to inquire if the mean color-gradient shown in Figure 2 applies equally to all absolute magnitudes, and to E and S0 galaxies separately. *A priori* one might expect a difference between E and S0 types. The former are pure spheroidal systems, while the latter contain a strong disk component. Hence, the formation histories of these two galaxy types have clearly been different in the *ratio of the collapse time to the time for first-generation star formation* (Sandage, Freeman, and Stokes 1970). In E galaxies (no disk) the star formation had to have been essentially complete *before* the gas in the collapsing protocloud could dissipate to a plane. On the other hand, in S0 systems (old disk galaxies), the gas did not change completely into stars in the collapse time (initial free-fall plus later dissipation near the disk); hence, a disk was formed from gas not used up in the halo-star formation.

Since there are observational reasons to believe that the disk in our galaxy has higher metal abundance than the halo, a natural mechanism could be imagined to explain why S0 *disks* might have a different radial chemical gradient from E *halos*. Hence, it is of interest to compare the observed color gradients in E and S0 galaxies separately.

The data, divided into E and S0 types, are shown in Figure 3. The solid curves are copied from Figure 2 and fit the data well, indicating that no gross differences exist in the color-aperture relation between E and S0 types.

Does the color-aperture relation depend on luminosity? The absolute magnitude of each galaxy in Figure 2 was computed from the redshift in Table 3 (using $H_0 = 50 \text{ km s}^{-1} \text{ Mpc}$) together with the listed V_{26} values. The sample was then divided into two groups; one from $-21.7 < M_V < -23.7$ [i.e., V mag between 8 and 10 as reduced to the Virgo cluster distance of $(m - M)_0 = 31.7$, using relative redshifts (see § VII)], and another from $-19.7 < M_V < -21.7$. The color-aperture relations of these two groups are shown in Figure 4, where the solid curves are the same as in Figure 2. The curves generally fit the data well, from which we conclude that the mean color-aperture relation is independent of the absolute magnitude, to within our accuracy.

Using these results, all data in Table 2 have been reduced to $\theta/D(0) = 0.5$ by applying equations (3)–(5). The average reduced colors for each galaxy are taken to represent the standard color $(u - V)_{0.5}$, $(b - V)_{0.5}$, $(V - r)_{0.5}$ for each galaxy. These colors are listed in Table 3, and discussed later.

Concerning these corrections, it should be noted that there is considerable scatter in Figure 4, especially in $\Delta(u - V)$ for the ellipticals. There are, in fact, a number of E galaxies with blue nuclei [i.e., negative

-0.14 in $u - V$, -0.09 in $b - V$ and -0.03 in $V - r$. But the difference is generally of small consequence in the reduction of Table 2 to the fully corrected Table 3 values. We only wish to note that Table 3 has not been corrected using the steeper UBV gradients. We also note that the aperture corrections in Paper I did use the larger UBV gradients.

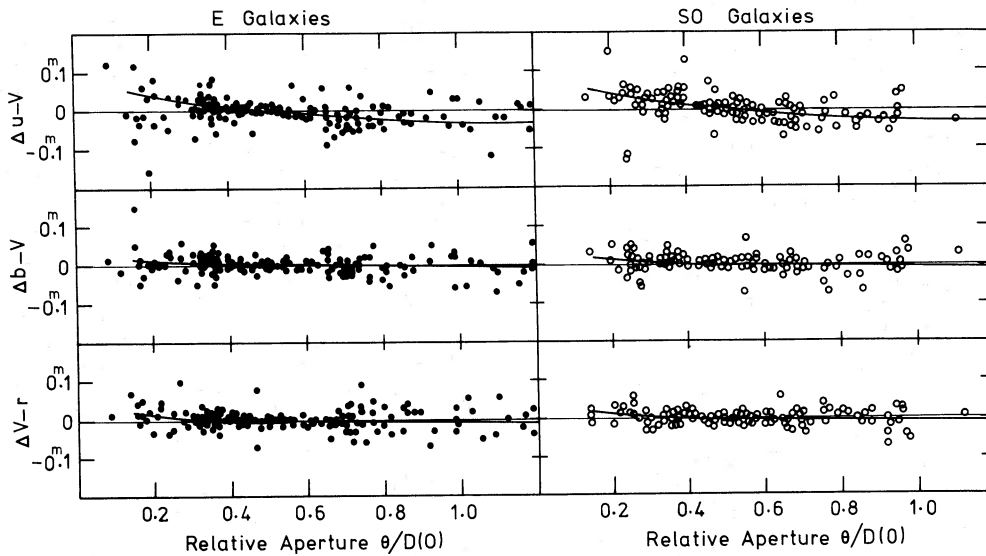


FIG. 3.—Color-aperture gradients in $u - V$, $b - V$, and $V - r$ from data in Table 2 separated into E and S0 types

$\Delta(u - V)$ values], a phenomenon that was noted earlier by de Vaucouleurs and by Tifft (references given earlier). But it should be emphasized that the effect on the corrections is usually small. Most of the galaxies here have been observed with large apertures [i.e., $\theta/D(0) \geq 0.3$; see Table 2]; hence the corrections to $\theta/D(0) = 0.5$ are also generally small, and the scatter in Figure 2 for E galaxies when $\theta/D(0) < 0.25$, although interesting as a separate problem, is of little consequence in this reduction.

What is the cause of the color gradient? Note that the ratio of the slopes in $\Delta(u - V)$, $\Delta(b - V)$, and $\Delta(V - r)$ (-0.10 , -0.03 , -0.03) is nearly the same as the ratio of those derived from the C-M relation in Paper I (-0.10 , -0.01 , -0.01). Hence, if the integrated C-M relation itself for whole galaxies is caused by the effects of abundance differences (Faber 1973, 1978), the *prima facie* case is strong that the gradient *within* a given galaxy is also caused by the same effect. The same conclusion has been reached

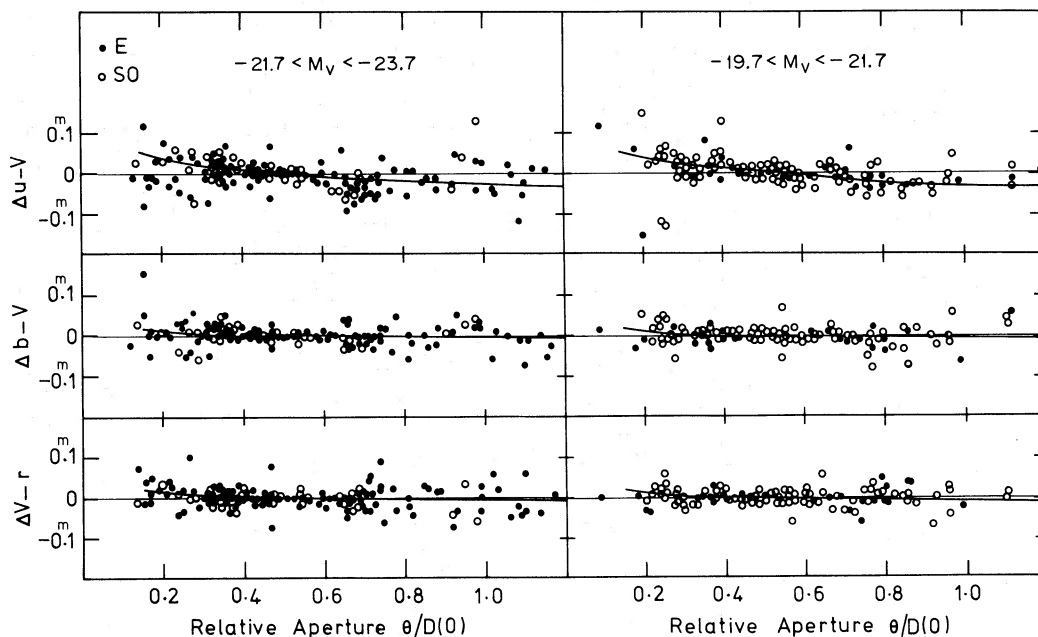


FIG. 4.—Color-aperture gradients in $u - V$, $b - V$, and $V - r$ from data in Table 2, separated into two absolute-magnitude intervals.

TABLE 3—Continued

Name (1)	I^H (2)	b^H (3)	L_{SG} (4)	B_{SG} (5)	Type (6)	v_H (7)	v_o (8)	Source (9)	V_{26} (10)	$(u-V)_{0.5}$ (11)	$(b-V)_{0.5}$ (12)	$(V-r)_{0.5}$ (13)	n (14)	Remarks (15)
IC 5181	350	-53.6	240	+14	SO ₁ (8)	+2110	+2082	E	11.18	2.30	0.57	0.53	1	N 7213 small group
NGC7252	28	-56.2	259	+26	SO or Gi H II	+4733	+4812	A	12.26	1.70	0.39	0.50	1	
NGC7302	48	-55.1	271	+29	+2586	+2714	+2714	A	12.25	2.34	0.56	0.50	1	
NGC7332	87	-29.7	315	+37	SO _{2/3} (9)	+1204	+1463	A	10.65	2.18	0.53	0.50	3	Pair w N 7339
NGC7377	36	-61.6	265	+22	SO _{2/3} /Sapec	+3416	+3499	A	11.49	2.30	0.63	0.44	1	
NGC7385	82	-41.3	301	+33	EO	+7829	+8053	A	12.73	2.68:	0.70:	0.63:	1	G 7385 HMS group, dominant
NGC7410	358	-62.8	250	+11	SBa(s)	+1638	+1633	I	10.34	-	IC 1459 Grus group
IC 5267	350	-61.8	247	+9	SO ₁ (4)/Sa	+1715	+1691	I	10.36	-	IC 1459 Grus group
IC 1459	5	-64.1	253	+13	E4	+1618	+1629	GI	10.06	2.42	0.60	0.52	3	IC 1459 Grus group, dominant
IC 5269	6	-64.3	254	+13	SO ₁ (7)	+2162	+2175	E	12.56	2.03	0.58	0.50	1	IC 1459 Grus group
NGC7457	96	-26.9	323	+32	SO ₁ (5)	+525	+791	A	11.08	2.15	0.56	0.49	1	
NGC7464	88	-39.4	307	+31	SO(4)	+1872	+2105	C	12.23	1.67:	0.50:	0.61:	1	Pair w N7465, Not SA
NGC7465	88	-39.4	307	+31	SO or S	+1994	+2227	C	13.34	1.55:	0.38:	0.48:	1	Pair w N 7464, Not SA
NGC7503	84	-47.6	298	+27	E1	+13,229	+13,429	A	13.41:	2.29:	0.82:	0.59:	1	Cluster, Not SA
NGC7507	23	-68.1	262	+14	EO	+1637	+1681	A	10.62	2.44	0.63	0.59	3	
NGC7562	85	-49.0	297	+26	E2	+3806	+4002	C	11.83	2.42	0.64	0.61	1	G 7619 HMS group, Not SA
NGC7576	74	-58.3	285	+22	Sa or SO ₃ :	+3572	+3725	AD	12.90	2.20:	0.57:	0.56:	1	Not SA
NGC7585	74	-58.4	285	+22	SO ₁ (3)/Sa	+3352	+3505	AC	11.56	2.32	0.59	0.49	4	
NGC7600	70	-60.6	282	+21	SO ₁ (5)	+3391	+3528	A	12.03	2.22	0.54	0.50	2	
NGC7617	88	-48.3	299	+25	E6	+4072	+4273	A	13.93	2.14	0.63	0.72	1	G 7619 HMS group, Not SA
NGC7619	88	-48.3	299	+25	E3	+3757	+3958	A	11.29	2.58	0.68	0.57	1	G 7619 HMS group
NGC7626	88	-48.4	299	+25	E1	+3357	+3558	A	11.26:	2.49	0.63	0.59	2	G 7619 HMS group
NGC7671	93	-45.4	304	+24	SO ₁ (5)	+4129	+4341	B	12.67	2.52	0.71	0.62	1	Not SA
NGC7679	87	-53.4	295	+22	Gi H II or SOpec	+5154	+5334	AB	12.66	1.18:	0.22:	0.69:	1	
IC 5328	339	-66.2	249	+3	E3	+3049	+3005	E	11.19	2.36	0.57	0.53	1	
NGC7702	323	-58.0	239	-2	Sa:	+3152	+3057	E	11.88	2.31:	0.62:	0.55:	2	
NGC7743	97	-49.5	302	+20	SBa	+1802	+1993	A	11.05	2.25	0.57	0.45	3	
NGC7744	339	-69.2	252	+2	SO ₁ (3)	+2990	+2952	E	11.38	2.41	0.60	0.51	1	
NGC7785	99	-54.3	299	+16	E5	+3846	+4020	A	11.85	2.55:	0.61:	0.59	1	
NGC7796	318	-60.1	241	-5	E2	+3461	+3361	EG	11.45	2.44	0.60	0.55	2	

with different data by Strom *et al.* (1976), and is supported by the fact that the abundance gradients exist in the spheroidal components of many bright nearby galaxies as well as in the disks of late-type spirals (Spinrad *et al.* 1971; Searle 1971; Trimble 1975; Audouze and Tinsley 1976).

The problem is discussed in more detail in Appendix A, where the observed integral color effect (eqs. [3]–[5]) is changed to a self-consistent smooth radial gradient whose integrals, weighted by the intensity gradient $I(r)$, give back equations (3)–(5). The surface variation of color can apparently be explained by a metal abundance gradient of a factor of ~ 2 over the interval $0.1 < \theta/D(0) < 1.0$.

b) *K-Reddening due to Redshift*

Shifting the galaxy spectrum under our fixed intermediate-band filters gives K terms that differ from the UBV values (Oke and Sandage 1968; Whitford 1971; Schild and Oke 1971 and references therein) due to our restricted bandwidths and different effective wavelengths. The K -reddening for our filter system has been calculated by shifting an internally derived energy distribution (obtained from the present observations of E galaxies in the Virgo and Coma clusters, reduced to zero redshift and averaged) through the $ubVr$ filter system. The adopted rest-energy distribution agrees well with those of Whitford (1971) and Schild and Oke (1971).

To an excellent approximation we find the K -redden-

ing in the $ubVr$ system over the velocity range of $0 < v < 12,000$ km s⁻¹ to be

$$K(u - V) = 0.4z \text{ mag}, \quad (6)$$

$$K(b - V) = 5.5z \text{ mag}, \quad (7)$$

and

$$K(V - r) = 2.2z \text{ mag}. \quad (8)$$

where $z \equiv \Delta\lambda/\lambda_0$.

Equations (6)–(8), together with the conventional K_V values (Whitford 1971, Table 3), have been used to correct data in Table 2 to the rest frame, as listed later in Table 3.

It should be noted that K_{u-V} corrections for most of the galaxies in Table 2 are usually negligible ($z < 0.01$) because our ultraviolet filters are narrow and away from the blanketing break in the galaxy spectrum at $\lambda = 4100$ Å. Hence, distance determinations of the local galaxies are little affected by the K correction.

On the other hand, in the case of $b - V$, the K correction is much larger than in $u - V$ because the b filter is narrow and is centered where the energy-distribution curve of galaxies has its maximum change of slope.

IV. APERTURE CORRECTION TO MAGNITUDES

The measured V magnitudes have been corrected to a standard fixed fraction of each galaxy's size by the method in HMS (Appendix A), using a growth

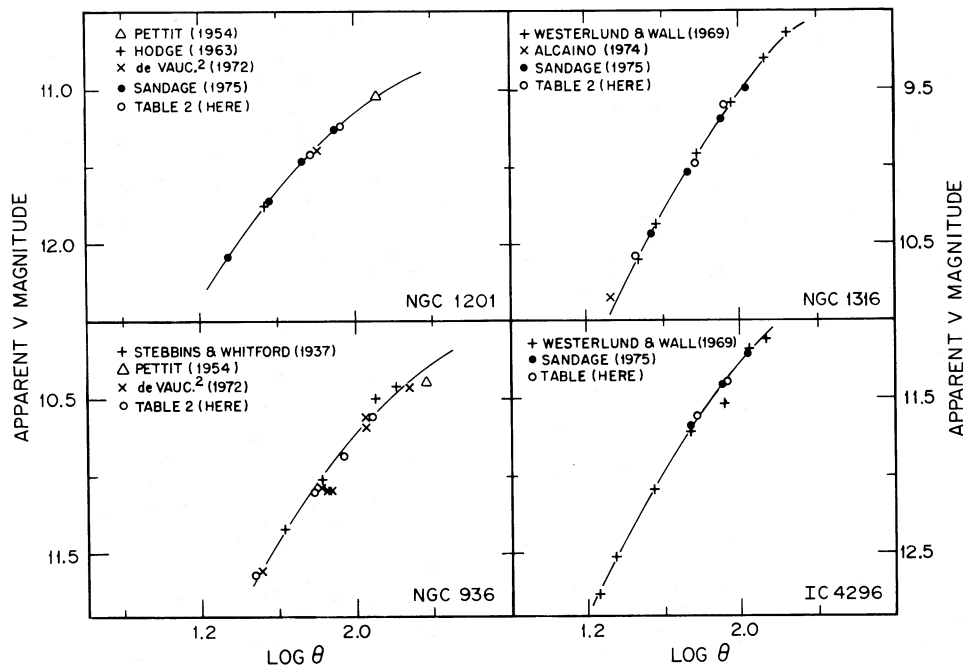


FIG. 5.—Representative growth curves using photoelectrically measured magnitudes from the indicated literature references, and for values listed in Table 2.

curve and the standard isophotal size adopted previously and listed elsewhere (Sandage 1975, Appendix B, Table B1) and discussed further in Appendix A here.

The observational material upon which final reduction to the standard isophotal magnitude V_{26} is based consists of the (V, θ) data in Table 2, plus other available photoelectric V magnitudes from the literature (Stebbins and Whitford 1937, 1952; Bigay 1951; Bigay and Dumont 1954; Pettit 1954; Holmberg 1958; Tift 1961; de Vaucouleurs 1961*b*; Hodge 1963; Webb 1964; Shobbrook 1966*b*; McClure and van den Bergh 1968; Westerlund and Wall 1969; de Vaucouleurs and de Vaucouleurs 1972; Alcaino 1974; Sandage 1972, 1973, 1975).

The available V magnitudes were plotted versus $\log \theta$ for each galaxy in Table 2 so as to form separate, partial growth curves. Examples are shown in Figure 5, where the shape of the standard curve has been put through the points by sliding in both coordinates for best fit.

Isophotal (V_{26}) magnitudes were then determined for each galaxy by three nearly independent methods, which, although almost equivalent, emphasize different aspects of the data.

1. Where many $(V, \log \theta)$ points are available, a sliding fit of the standard² growth-curve template can be made without knowledge of the intrinsic (reduced for inclination) galaxy diameter $D(0)$. The

² We find that the growth curve is similar, to within the errors, for E and S0 galaxies, and also for different absolute magnitudes; hence, one standard growth-curve template was used for all the galaxies.

corrected magnitude, V_{26} , read at the marked standard size of $2.5 D(0)$, is accurate as long as many V, θ points are available. However, when only few data are available, the method used by HMS (Appendix A) is required.

2. When $D(0)$ is known for any given galaxy, each (V, θ) pair can be corrected, using the standard growth curve. Two lists of intrinsic galaxy diameters are available. (a) The $D(0)$ values that are given in RCBC (1st ed.) are adopted as listed, and have been used to form $\theta/2.5 D(0)$, i.e., the argument of the adopted growth curve. (b) An independent estimate of galaxy diameters was made in 1955 from the original *National Geographic Society-Palomar Sky Survey* Schmidt plates, as the Sky Survey was in progress. These diameters, θ_s , had been previously used by one of us (but not published) for the aperture corrections in HMS. Similar diameters on the same scale have been estimated more recently for many southern galaxies in the sample from Uppsala Schmidt plates (designated here by subscript u) taken between 1969 and 1972 at Mount Stromlo for the present work. Comparison shows $\theta/2.5 D(0) \approx \theta/3.1 \theta_s \approx \theta/3.1 \theta_u$; hence the standard growth curve can again be entered in the $\theta/2.5 D(0)$ argument to find V_{26} .

The mean of the V_{26} values, obtained in these three ways, has been adopted. Comparison of the distribution of differences in V from the mean for each method gives $\sigma(\Delta V_{26}) \approx \pm 0.1$ mag, which, being much larger than the individual measuring errors of $\sigma(V) \lesssim \pm 0.02$ mag, shows the accuracy of our reduction procedure rather than the errors of the observations themselves.

V. TYPES, VELOCITIES, STANDARD VISUAL MAGNITUDES AND CORRECTED COLORS OF PROGRAM GALAXIES

The photometric data corrected using the foregoing precepts, along with the new types and velocities for the 405 program galaxies, are given in Table 3.

Column (1) lists the NGC or IC members; columns (2)–(5) show the galactic and supergalactic coordinates taken from the RCBG; column (6) lists again the revised types taken from Table 2; column (7) is the observed heliocentric velocity V_H from sources in the literature or from new measurements discussed in detail elsewhere (Sandage 1978); column (8) is V_H from column (7), corrected for the standard solar motion relative to the Local Group of $300 \sin l \cos b$ km s⁻¹ used by HMS; in column (9) are sources for the velocity V_H as listed in the next paragraph; column (10) shows the derived V_{26} magnitudes (§ IV); uncertain magnitudes are indicated with colons. Columns (11)–(13) show the colors in Table 2 (cols. [7], [8], [9]) reduced to $\theta/D(0) = 0.5$ by applying equations (3)–(5) and labeled $(u - V)_{0.5}$, $(b - V)_{0.5}$, and $(V - r)_{0.5}$. Where more than one corrected value is available, the means are given. [If the color is uncertain for all the apertures, the resulting color at $\theta/D(0) = 0.5$ is marked with a colon.] Column (14) shows the number of observations used to derive the means in columns (11)–(13). In column (15), cluster and group members and non-Shapley-Ames members are identified. Galaxies that appear to be isolated by many apparent diameters (≥ 100) from neighbors of about the same magnitude and size are assigned to field, but are not so designated in column (15).

The sources for the observed velocities are: (A) Humason in HMS; (B) Mayall in HMS; (C) de Vaucouleurs and de Vaucouleurs (1961); (D) Mayall and de Vaucouleurs (1962); (E) new here, some of which are published in Sandage (1975) but with a systematic difference of 30 km s⁻¹ smaller there as explained elsewhere (Sandage 1978); (F) de Vaucouleurs and de Vaucouleurs (1967) and de Vaucouleurs (1960, 1961a); (G) Evans (1963); (H) Catchpole, Evans, and Jones (1969); (I) Shobbrook (1966a); (J) Evans and Malin (1965); (K) Kintner (1971); (L) Sargent (1970); (M) Smith (1972); and (N) Page (1970).

VI. THE MEAN GALACTIC REDDENING FOR THIS SAMPLE

Two models for local galactic reddening are current, but at the moment there is no general agreement on how to resolve their differences. Galaxy counts (Hubble 1934; Shane and Wirtanen 1954, 1967; de Vaucouleurs and Malik 1969; Noonan 1971; Holmberg 1974; Heiles 1975) show the steep gradient $\Delta \log N(m)/\Delta \text{csc } b \gtrsim 0.15$ for galactic latitudes below $b \approx 30^\circ$ ($\text{csc } b = 2$). If a uniform plane-parallel model for the absorption is assumed, then an extrapolation to the pole with this slope gives an extinction of $A_B \gtrsim 0.25$ mag.

However, the idealization of a uniform model would be unjustified if the extinction occurs predominantly in clouds. Noonan (1971) makes the point

that in the cloud model, counts above $|b| \approx 45^\circ$ need not be related to those at lower latitudes (which contribute most to the determination of the slope). A broken cumulus terrestrial sky provides a commonplace analogy. Although the clouds are actually uniformly spaced in the atmosphere, they appear to crowd toward the horizon because zones of equal $\Delta \text{sec } z$ (equal air mass) are not zones of equal differences in zenith distance. Hence, the zenith is mostly clear, although the horizon is not.

In support of the cloud model, the direct evidence for nearly zero reddening in the galactic poles comes from studies of individual stars and star clusters by Eggen and Sandage [1965, $E(B - V) < 0.03$], McClure and Racine (1969, 0.00), Crawford and Barnes (1969a, b; 0.01), McNamara and Longford (1969, < 0.01), Gottlieb and Upson (1969, < 0.01), Sandage (1969, 0.00 for M3; 0.02 for M92), Helfer and Sturch (1970, 0.00), Peterson (1970, 0.03), McClure and Crawford (1971, 0.00), Philip and Tiftt (1971, 0.00), Feltz (1972, 0.00), Knapp (1975, 0.008), Appenzeller (1975, < 0.01), Burstein and McDonald (1975, 0.03), and others.

The present color data for the homogeneous E and S0 galaxy types permit still another determination of mean reddening with galactic latitude. Because corrected $(V - r)_{0.5}^K$ colors are nearly independent of M_V (Paper I, Fig. 3), their correlation with $\text{csc } b$ measures the mean reddening. A check can be made using the $(b - V)_{0.5}^K$ and $(u - V)_{0.5}^K$ colors as well, corrected to $M_V = -22$ for each galaxy by the calibration of Paper I, with M_V calculated for each galaxy from $H_0 = 50 \text{ km s}^{-1} \text{ Mpc}^{-1}$.

The results for $b - V$ and $V - r$ colors, shown in Figure 6, give the shallow correlations, determined by eye,

$$\Delta(b - V)_{0.5}^{K, -22} = 0.033 \Delta \text{csc } b, \quad (9)$$

$$\Delta(V - r)_{0.5}^K = 0.026 \Delta \text{csc } b. \quad (10)$$

(Least-squares solutions were not made because of the obvious nonuniform distribution of points in $\text{csc } b$.)

The slope of equation (9) is the same as found earlier from a different sample (Sandage 1973, § IV). Moreover, the ratio $E(b - V)/E(V - r) = 1.3$ here is close to that given by the standard reddening curve (cf. Whitford 1958; Nandy 1964).

There is, however, some suggestion from Figure 6 that the $V - r$ colors are not well represented by equation (10) in the interval $50^\circ < b < 90^\circ$, but rather that these colors define a steeper relation in these latitudes, contrary to the requirement of the reddening-free polar cap model. But we are unconvinced of the reality of a steep $V - r$ slope for $b > 50^\circ$ for two reasons. (1) The small color excess for polar cap stars determined from the large number of studies quoted at the beginning of this section seems definitive to us. (2) Our data for $(u - V)_{0.5}^{K, M}$ also suggest a reddening-free polar region. Plotted in Figure 7 is the fully reduced $u - V$ color (corrected for color gradient, K , and absolute magnitude effect) versus $\text{csc } b$ in the latitude

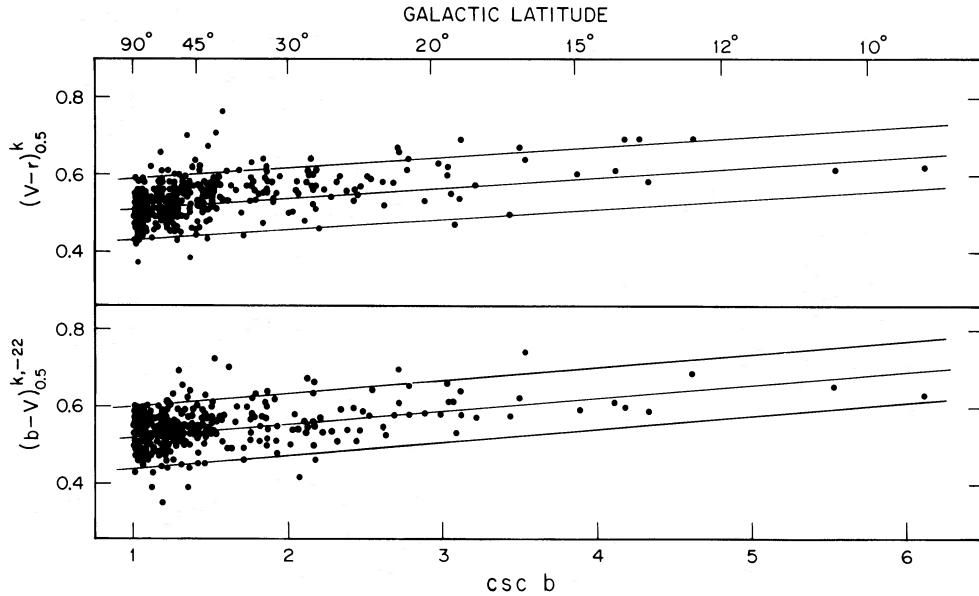


FIG. 6.—Correlation of $\csc b$ with $b - V$ and $V - r$ colors corrected to $\theta/D(0) = 0.5$, for K -dimming, and to $M_V = -22$ (for $b - V$), for the Shapley-Ames galaxies in our sample.

interval $50^\circ < b < 90^\circ$. For an extinction of $A_V \gtrsim 0.25$ mag required by the galaxy counts (extrapolated to the pole as if the low-latitude and polar counts *can* be connected), the expected gradient in $u - V$ would be $\gtrsim 0.15 \Delta \csc b$ or $\Delta(u - V) \gtrsim 0.04$ mag over the interval in Figure 7 of $1 \leq \csc b < 1.3$, which clearly is not present here. Hence, Figure 7 does not confirm the indicated steeper slope in $(V - r)_{0.5}^K$ and, in fact, shows no positive slope at all. Hence, we keep the polar absorption-free model. The complete $(u - V)_{0.5}^K$ versus $\csc b$ diagram is given in Figure 8, which shows again the general shallow slope (0.063) to the mean $u - V$ reddening versus $\csc b$ relation over the observed latitude interval $90^\circ > b > 10^\circ$.

The slopes from Figures 6 and 8 are smaller by a factor of 2 than those inferred using intermediate-latitude galaxy counts. From this result and in view of the strong evidence for small $E(B - V)$ values in the pole, principally from the stellar data, we accept a mean cloud model and adopt

$$E(b - V) = 0.033(\csc b - 1) \quad \text{for } |b| < 40^\circ, \quad (11)$$

$$E(b - V) = 0 \quad |b| > 50^\circ,$$

$$E(V - r) = 0.026(\csc b - 1) \quad \text{for } |b| < 40^\circ, \quad (12)$$

$$E(V - r) = 0 \quad |b| > 50^\circ,$$

$$E(u - V) = 0.063(\csc b - 1) \quad \text{for } |b| < 40^\circ, \quad (13)$$

$$E(u - V) = 0 \quad |b| > 50^\circ,$$

$$A_V = 0.10(\csc b - 1) \quad \text{for } |b| < 40^\circ, \quad (14)$$

$$A_V = 0 \quad |b| > 50^\circ,$$

with a smooth transition from $40^\circ < |b| < 50^\circ$ to avoid a step.

Finally, we should caution that equations (11)–(14) apply to our *magnitude-limited* sample. The slope coefficients are smaller than those which would apply to a distance-limited sample since highly reddened galaxies with large A_V are lost to the Shapley-Ames listing because they are extinguished below the catalog limit. However, equations (11)–(14) are appropriate to the present sample.

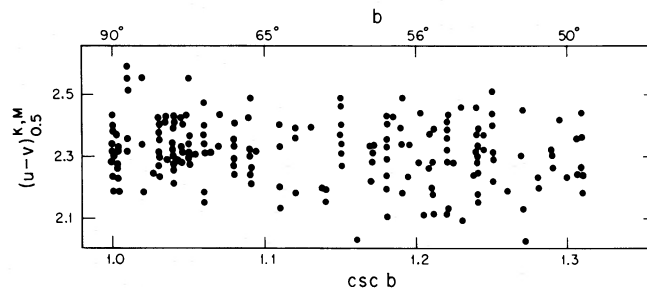


FIG. 7.—The $u - V$ colors corrected for color gradient, K term, and absolute-magnitude effect for galaxies from Table 3 in the latitude interval $90^\circ > b > 50^\circ$.

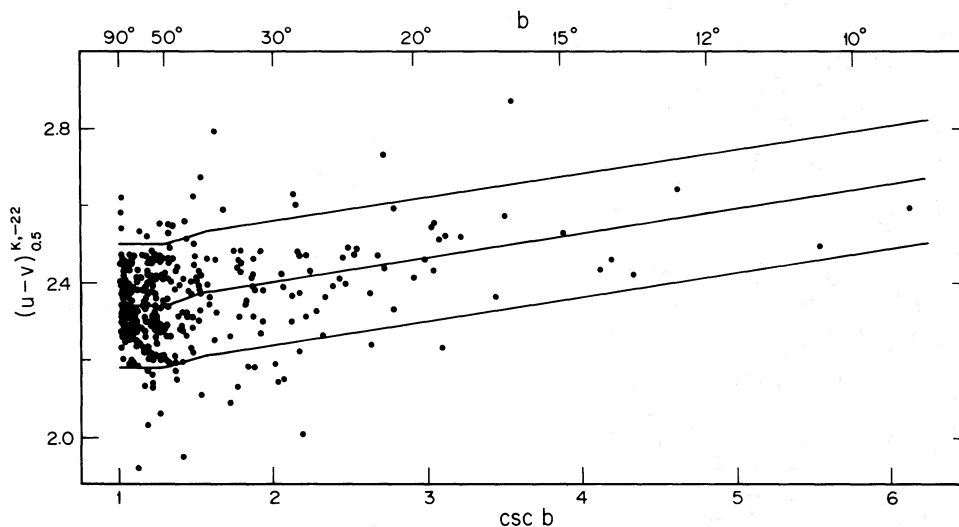


FIG. 8.—Same as Fig. 6 for corrected $u - V$ colors. The slope of the ridge and envelope lines for $b < 40^\circ$ is 0.063 as in eq. (13) of the text. The larger scatter than in Fig. 6 is undoubtedly due to intrinsic variations rather than to spotty reddening.

VII. C-M RELATION FOR FIELD GALAXIES

In Paper I, we found that the C-M relation for E and S0 galaxies in Virgo was well defined. Further, the cluster relation was shown to fit the composite C-M relation of nine other groups and clusters, formed by shifting the individual V_{26} magnitudes to the Virgo cluster distance by the ratio of the redshifts. This tests the universality and absolute zero-point of the C-M relation for these particular clusters and groups.

In this section, we construct a similar composite C-M relation for isolated E and S0 galaxies, again reduced to the Virgo cluster distance by the ratio of the redshifts, to test if the C-M relation of Virgo applies to field galaxies as well. For each field galaxy, zero-point shifts in magnitude, $\Delta(m - M)_0$, relative to Virgo cluster were computed from $5 \log v_0/v_{\text{VIRGO}}$, where v_0 is the redshift of the field galaxy, and $v_{\text{VIRGO}} = 1100 \text{ km s}^{-1}$. The magnitudes, reduced to Virgo (V_{26}°)_{VIRGO}, were computed for each field galaxy by subtracting $\Delta(m - M)_0$ from V_{26}° . All the galaxies which are not cluster or group members in Table 3 are taken to be field galaxies. Further, all field galaxies of types Sa and later, as well as galaxies with high errors in colors, have been omitted. Although the ultimate purpose of the present series of papers is to test the regularity of the velocity field by the reverse argument, it is known that the perturbations on a Hubble flow, if they exist, are certainly less than 500 km s^{-1} for local galaxies (i.e., galaxies with $v_0 \lesssim 2000 \text{ km s}^{-1}$) (cf. Sandage 1975; Tammann and Kraan 1978). Hence, errors in our calculated magnitudes at Virgo, obtained from the measured velocities, are certainly less than $\delta M = 2.17 \Delta v/v \lesssim 1 \text{ mag}$, which is sufficiently small to make this a useful comparison of the field and cluster C-M relations. It is also known that the systematic velocity of $v_0 = 1100 \text{ km s}^{-1}$ for

Virgo is consistent with a completely quiet Hubble flow (Sandage and Tammann 1974, 1975; Paper I; Kormendy 1977); hence no systematic offset relative to Virgo will result in the C-M diagram for field galaxies by using this reduction procedure.

The resulting composite C-M relations of color versus $(V_{26}^\circ)_{\text{VIRGO}}$ are shown in Figure 9 for E and S0 galaxies separately. The ridge lines and the 2σ envelopes of the Virgo cluster C-M relations have been transferred directly from Paper I.

The field S0 galaxies fall within the $\pm 2\sigma$ lines in all three colors with only a few exceptions. Especially to be noted are the colors of N2787, which are much redder in $(u - V)_c$ and $(b - V)_c$, and probably indicating too low a correction for galactic reddening. Otherwise, the $(u - V)_c$ colors of the seven other galaxies that fall outside the 2σ lines are equally distributed on both the blue and red side, and are within $\pm 3\sigma$ of the ridge-line. There is a slight (0.03 mag) effect of the ridge line to the blue side of the data in $(b - V)_c$ for S0 galaxies. As the effect is not present in $V - r$ or $u - V$, and as our narrow b band is sensitive to the K term and to the severe blanketing effects near $\lambda 4100$, we question the reality of the small difference.

The field E galaxies also generally lie within the 2σ lines in $(b - V)_c$ and $(V - r)_c$, with very few exceptions. But in the $(u - V)_c$ C-M relation, 22 galaxies lie outside $\pm 2\sigma$; 15 lie on the blue side and seven fall to the red. Of these, NGC 1400 is much redder and NGC 3156 is much bluer than the mean C-M relation. Although a larger value of $\sigma_{u-V} = \pm 0.08 \text{ mag}$ (compared with $\sigma_{u-V} = \pm 0.06$ for Virgo) could cover most of the galaxies within $\pm 2\sigma$, the excessive number of galaxies in the blue side of the 2σ line in Figure 7 could be due to (1) misclassification (E galaxies can be more easily misclassified than S0 on poor plates); (2) episodes of more recent star

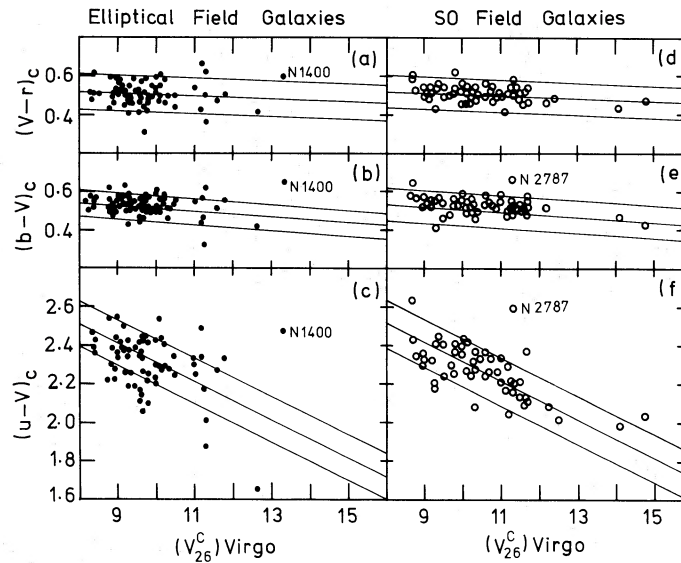


FIG. 9.—The color-magnitude relation for field (isolated) E and S0 galaxies from Table 3, reduced to the distance of the Virgo cluster. The ridge line and the $\pm 2\sigma$ envelope lines are from the Virgo cluster calibration of Paper I.

formation such as in NGC 205 (Baade 1950); (3) too large a reddening correction for galaxies in low galactic latitudes; and (4) a true perturbation in the velocity field, making our $\Delta(m - M)_0$ values systematically incorrect for some galaxies.

Although investigation of the last possibility is one of the main purposes of this series, we note here in passing that the 11 E galaxies that lie most strongly blueward of the lower envelope of Figure 7c (IC 2035, NGC 1638, 2865, 2924, 3156, 4742, 5322, 5493, 6854, 7079, 7192) are spread rather uniformly over the sky (Fig. 1), and hence their deviations cannot be explained by velocity perturbations. Concerning points (1) and (3), we can note that the classification of IC 2035 is uncertain (it has a high surface brightness and could be an unresolved H II-region galaxy), and that NGC 1638, 2865, 2924 and 6854, which are in low galactic latitude, do show larger deviations in Figure 7c.

Our conclusion from Figure 7 is that the C-M relation for field E and S0 galaxies is closely the same as for galaxies in clusters and groups, but probably has a larger scatter ($\sigma_{u-v} = \pm 0.08$ mag). Hence the C-M

effect can be used in the case of field galaxies to improve estimates of the absolute magnitude M_V and, through this, to obtain better distances compared to those made with no knowledge of colors.

Finally, we should mention that the agreement of the C-M effect for galaxies inside and outside of clusters and between E and S0 galaxies separately does not support speculations that the stellar content and evolutionary development of galaxies depends more on their environment than on the initial conditions at their formation, a problem that is discussed in Paper III.

This work has been partially supported by grant MPS 72-05099 from the National Science Foundation and by special funds from the Carnegie Institution of Washington. We are also grateful to Jay Frogel and Eric Persson for showing us their *UBVR* color data for a number of galaxies in common with Table 2, which permitted a comparison of the color systems and the color-aperture gradients.

APPENDIX A

VARIATION OF SURFACE COLOR WITH RADIUS DERIVED FROM APERTURE PHOTOMETRY

The variation of surface color with radius cannot be obtained uniquely from the integral (aperture) gradients (eqs. [3]–[5] of the text) because many *unsmooth* color = $f[\theta/D(0)]$ functions can produce them to within the errors. However, a self-consistent *smooth* variation of $u - V$, $b - V$, and $V - r$ colors with $\theta/D(0)$ can be calculated by numerical differencing of the relevant data, because the aperture color is the difference between the integrated magnitudes at a given $\theta/D(0)$ in two wavelengths.

The existence of a color gradient means that the shape of the growth curve $\Delta \text{mag} = f[\theta/D(0)]$ depends on wavelength. Hence the luminosity profile, $I(r)$, must also be wavelength-dependent. However, for the purposes of

this Appendix we need not know the functional form of $I(r, \lambda)$, but only its integral, i.e., the growth curve itself in each color.

The adopted growth curve in V is the same as used in § IV. It is smoothed analytically here using a cubic in the interval $-1 < \log \theta/D(0) < +0.9$. The curve, renormalized to $\Delta m = 0$, at $\theta/D(0) = 0.5$, is well represented by

$$\Delta m = -0.449 - 1.291 \log \theta/D(0) + 0.667[\log \theta/D(0)]^2. \quad (\text{A1})$$

The curves in u , b , and r can now be obtained from equation (A1) by adding the appropriate magnitudes from equations (3)–(5) of the text. The resulting u , b , and r curves naturally have different shapes, and it is these differences that contain the color gradient implicitly. Because the curves are now analytical, based on equations (3), (4), (5), and (A1), they are smooth at any arbitrary level; therefore, numerical differentiation can be precise. The color at any given radius can now be obtained as follows.

The intensity within a radius r_i in the V bandpass is

$$I_V(i) = \text{dex} [-0.4 \Delta m_V(i)], \quad (\text{A2})$$

where $\Delta m_V(i)$ is given by equation (A1), with $r_i \equiv \theta_i/D(0)$.

The intensity in an *annulus*, bounded by radii r_i and r_j ($r_i > r_j$ by convention) is then

$$I_V(ij) = \text{dex} [-0.4 \Delta m_V(i)] - \text{dex} [-0.4 \Delta m_V(j)]. \quad (\text{A3})$$

The color of the annulus follows directly from the definition of magnitudes as

$$(u - V)_{ij} \equiv 2.5 \log (I_V/I_u) = 2.5 \log \left\{ \frac{\text{dex} [-0.4 \Delta m_V(i)] - \text{dex} [-0.4 \Delta m_V(j)]}{\text{dex} [-0.4 \Delta m_u(i)] - \text{dex} [-0.4 \Delta m_u(j)]} \right\}. \quad (\text{A4})$$

Equation (A4) solves the problem because all quantities on the right are known at any pair of radii r_{ij} from the separate growth curves based on equations (3), (4), (5), and (A1). Similar expressions exist for $b - V$ and $V - r$.

The results of equation (A4) and the similar equations in b and r , when they are applied to the aperture gradients of equations (3)–(5) (§ IIIa), give surface color gradients over the interval $0.1 \lesssim \theta/D(0) \lesssim 1$ as

$$\Delta(u - V) \propto 0.15 \log \theta/D(0), \quad (\text{A5})$$

$$\Delta(b - V) \propto 0.05 \log \theta/D(0), \quad (\text{A6})$$

$$\Delta(V - r) \propto 0.05 \log \theta/D(0), \quad (\text{A7})$$

as obtained by numerical curve fitting. (If the UBV literature gradients are used, rather than the adopted values from eqs. [3]–[5], the coefficients of eqs. [A5]–[A7] are 0.20, 0.13, and 0.04, respectively.)

Naturally, these rates are steeper than those in equations (3)–(5) because of contamination of the annular colors by light from the interior regions in the aperture photometry. For disk galaxies, these rates, which are ~ 1.5 times greater than the aperture rates, should represent the radial change of color and hence the change of mean metal abundance with θ , when calibrated. For halo systems, the true spatial gradient will again be steeper because the spot values are themselves projections on the sky of integrations through the galaxian geometry.

Lower limits on the true variation of Fe/H with r can therefore be put using equations (A5)–(A7) and the preliminary calibration by Strom *et al.* (1976). These authors used classical considerations of the position of giant and subgiant sequences in the C-M diagram as a function of Fe/H, folded them with the appropriate luminosity functions, and integrated in several colors for the total light, to obtain

$$\Delta(V - K) \approx 0.85 [\text{Fe}/\text{H}]. \quad (\text{A8})$$

From unpublished work by Frogel and Persson, the amplitude of the C-M effect is closely the same in $V - K$ as in $u - V$ colors, hence equations (A5) and (A8) require

$$\Delta[\text{Fe}/\text{H}] \approx 0.18 \log \theta/D(0) \quad (\text{A9})$$

for $0.1 < \theta/D(0) < 1$, which gives a metal-abundance variation of about a factor of 1.5 for θ between about 3 and 30 kpc [recall that $2.5 D(0) \approx 85$ kpc for first-ranked cluster ellipticals]. The variation in halo galaxies (i.e., E systems) could be steeper by another factor of 2 over the stated diameter interval, which then gives a mean abundance gradient of perhaps a factor 3 in this inner region. Spot photometry to test these predictions will be of clear importance.

REFERENCES

- Alcaino, G. 1974, *Astr. Ap. Suppl.*, **13**, 305.
 Appenzeller, I. 1975, *Astr. Ap.*, **38**, 313.
 Audouze, J., and Tinsley, B. M. 1976, *Ann. Rev. Astr. Ap.*, **14**, 43.
 Baade, W. 1950, *Pub. Obs. Univ. Michigan*, **10**, 7.
 Bigay, J. H. 1951, *Ann. d'Ap.*, **14**, 319.
 Bigay, J. H., and Dumont, R. 1954, *Ann. d'Ap.*, **17**, 78.
 Burstein, D., and McDonald, L. H. 1975, *A.J.*, **80**, 17.
 Catchpole, R. M., Evans, D. S., and Jones, D. H. P. 1969, *Observatory*, **89**, 21.
 Crawford, D. L., and Barnes, J. V. 1969a, *A.J.*, **74**, 407.
 ———. 1969b, *A.J.*, **74**, 1008.
 de Vaucouleurs, G. 1960, *Ap. J.*, **131**, 265.
 ———. 1961a, *Ap. J.*, **133**, 405.
 ———. 1961b, *Ap. J. Suppl.*, **5**, 233.
 de Vaucouleurs, G., and de Vaucouleurs, A. 1961, *Mem. R.A.S.*, **68**, 69.
 ———. 1964, *Reference Catalogue of Bright Galaxies* (Austin: University of Texas Press) (RCGB).
 ———. 1967, *A.J.*, **72**, 730.
 ———. 1972, *Mem. R.A.S.*, **77**, 1.
 de Vaucouleurs, G., and Malik, G. M. 1969, *M.N.R.A.S.*, **142**, 387.
 Eggen, O. J., and Sandage, A. 1965, *Ap. J.*, **141**, 821.
 Evans, D. S. 1963, *M.N.A.S. So. Africa*, **22**, 1963.
 Evans, D. S., and Malin, S. R. 1965, *M.N.A.S. So. Africa*, **24**, 32.
 Faber, S. M. 1973, *Ap. J.*, **179**, 731.
 ———. 1978, *Ap. J.*, in preparation.
 Feltz, K. A. 1972, *Pub. A.S.P.*, **84**, 497.
 Frogel, J., and Persson, E. 1977, private communication.
 Gottlieb, D. M., and Upson, W. L. 1969, *Ap. J.*, **157**, 611.
 Heiles, C. 1975, *Ap. J.*, **204**, 379.
 Helfer, H. L., and Sturch, C. 1970, *A.J.*, **75**, 971.
 Hodge, P. M. 1963, *A.J.*, **68**, 237.
 Holmberg, E. 1958, *Medd. Lund Obs.*, 2d Ser., No. 136.
 ———. 1974, *Astr. Ap.*, **35**, 121.
 Hubble, E. 1934, *Ap. J.*, **79**, 8.
 Humason, M. L., Mayall, N. U., and Sandage, A. 1956, *A.J.*, **61**, 97 (HMS).
 Johnson, H. L., and Morgan, W. W. 1953, *Ap. J.*, **117**, 113.
 Kintner, E. C. 1971, *A.J.*, **76**, 409.
 Knapp, G. R. 1975, *A.J.*, **80**, 111.
 Kormendy, J. 1977, *Ap. J.*, **218**, 333.
 Mayall, N. U., and de Vaucouleurs, A. 1962, *A.J.*, **67**, 363.
 McClure, R. D., and Crawford, D. L. 1971, *A.J.*, **76**, 31.
 McClure, R. D., and Racine, R. 1969, *A.J.*, **74**, 1000.
 McClure, R. D., and van den Bergh, S. 1968, *A.J.*, **73**, 1008.
 McNamara, D. H., and Longford, W. R. 1969, *Pub. A.S.P.*, **81**, 141.
 Nandy, K. 1964, *Pub. Roy. Obs. Edinburgh*, **3**, No. 6.
 Noonan, T. W. 1971, *A.J.*, **76**, 190.
 Oke, J. B., and Sandage, A. 1968, *Ap. J.*, **154**, 21.
 Page, T. 1970, *Ap. J.*, **159**, 791.
 Peebles, P. J. E. 1976, *Ap. J.*, **205**, 318.
 Peterson, B. A. 1970, *A.J.*, **76**, 695.
 Pettit, E. 1954, *Ap. J.*, **120**, 413.
 Philip, A. G. D., and Tift, L. E. 1971, *A.J.*, **76**, 567.
 Rood, H. J., and Baum, W. A. 1967, *A.J.*, **72**, 398.
 Sandage, A. 1961, *Hubble Atlas of Galaxies* (Washington: Carnegie Institution of Washington).
 ———. 1969, *Ap. J.*, **157**, 515.
 ———. 1972, *Ap. J.*, **178**, 1.
 ———. 1973, *Ap. J.*, **183**, 711.
 ———. 1975, *Ap. J.*, **202**, 563.
 ———. 1978, *A.J.*, **83**, in press.
 Sandage, A., Freeman, K. C., and Stokes, N. R. 1970, *Ap. J.*, **160**, 831.
 Sandage, A., and Tammann, G. A. 1974, *Ap. J.*, **194**, 559.
 ———. 1975, *Ap. J.*, **196**, 313.
 Sandage, A., Tammann, G. A., and Hardy, E. 1972, *Ap. J.*, **172**, 253.
 Sargent, W. L. W. 1970, *Ap. J.*, **160**, 405.
 Schild, R., and Oke, J. B. 1971, *Ap. J.*, **169**, 209.
 Searle, L. 1971, *Ap. J.*, **168**, 41.
 Shane, C. D., and Wirtanen, C. A. 1954, *A.J.*, **59**, 285.
 ———. 1967, *Lick Obs. Bull.*, **22**, 1.
 Shapley, H., and Ames, A. A. 1932, *Harvard Ann.*, **88**, No. 2.
 Shobbrook, R. 1966a, *M.N.R.A.S.*, **131**, 293.
 ———. 1966b, *M.N.R.A.S.*, **131**, 351.
 Silk, J. 1974, *Ap. J.*, **193**, 525.
 Smith, M. G. 1972, *Bull. AAS*, **4**, 237; and private communication.
 Spinrad, H., Gunn, J. E., Taylor, B. J., McClure, R. D., and Young, J. W. 1971, *Ap. J.*, **164**, 11.
 Stebbins, J., and Whitford, A. E. 1937, *Ap. J.*, **86**, 247.
 ———. 1952, *Ap. J.*, **115**, 284.
 Strom, S. E., Strom, K. M., Good, J. W., Vrba, F. J., and Rice, W. 1976, *Ap. J.*, **204**, 684.
 Tammann, G. A., and Kraan, R. 1978, *IAU Symposium No. 79, The Large-Scale Structure of the Universe*, ed. J. Einasto and M. S. Longair (Dordrecht: Reidel).
 Tift, W. G. 1961, *A.J.*, **66**, 390.
 ———. 1963, *A.J.*, **68**, 302.
 ———. 1969, *A.J.*, **74**, 354.
 Trimble, V. 1975, *Rev. Mod. Phys.*, **47**, 877.
 Visvanathan, N. 1972, *Pub. A.S.P.*, **84**, 248.
 Visvanathan, N., and Griersmith, D. 1977, *Astr. Ap.*, **59**, 317.
 Visvanathan, N., and Sandage, A. 1977, *Ap. J.*, **216**, 214 (Paper I).
 Webb, C. J. 1964, *A.J.*, **69**, 442.
 Westerlund, B. E., and Wall, J. V. 1969, *A.J.*, **74**, 335.
 Whitford, A. E. 1958, *A.J.*, **63**, 201.
 ———. 1971, *Ap. J.*, **169**, 215.

ALLAN SANDAGE: Hale Observatories, 813 Santa Barbara Street, Pasadena, CA 91101

NATARAJAN VISVANATHAN: Mount Stromlo and Siding Spring Observatories, Private Bag, Woden, A.C.T. 2606, Australia